J. Fluid Mech. (1975), *vol.* 72, *part* 2, *pp.* 391–399
Printed in Great Britain

Experimental investigations of cavitation-bubble collapse in the neighbourhood of a solid boundary

By W. LAUTERBORN AND H. BOLLE
Drittes Physikalisches Institut, University of Göttingen, West Germany

(Received 6 November 1974 and in revised form 31 March 1975)

Cavitation bubbles were produced by focusing giant pulses of a Q-switched ruby laser into distilled water. The dynamics of the bubbles in the neighbourhood of a solid boundary were studied by means of high-speed photography using a rotating-mirror camera with framing rates of up to 300000 frames/s. Bubble motion was evaluated from the frames with the aid of a digital computer using a graphical input device. Smoothed distance–time curves of different portions of the bubble wall were obtained also, allowing a reliable calculation of bubble-wall velocities (except at the actual instant of collapse). One of the numerical examples of the collapse of a spherical bubble near a plane solid boundary obtained by Plesset & Chapman could be realized experimentally. A comparison of the bubble shapes shows good agreement.

1. Introduction

The interest in the dynamics of cavitation bubbles in liquids, especially water, mainly arises from their destructive action on solid surfaces. But even the problem of how a single spherical cavitation bubble may collapse when near a solid surface could be studied directly neither theoretically nor experimentally until very recently (Plesset & Chapman 1971; Lauterborn 1974*a*, *b*; Bolle 1974).

Concerning theory, the difficulty arises from the lack of spherical symmetry of the problem. It seems that only numerical methods are capable of predicting bubble behaviour near the final stages of collapse. Plesset & Chapman (1971) were the first to calculate the liquid jet developing through the bubble towards the surface on collapse of an empty spherical bubble nearby.

Experimental investigations, on the other hand, suffer from the fact that the appearance of a cavitation bubble in real situations and even in most experimental environments is of a statistical nature both in location and time. Model cavitation bubbles produced by sophisticated methods seem now to be of greatest help in pushing our knowledge ahead. Using specially prepared bubbles, Naudé & Ellis (1961) and Benjamin & Ellis (1966) were able to show that jets may develop on bubbles collapsing near a solid surface. These studies strongly supported the idea, first put forward by Kornfeld & Suvorov (1944), that the damage to solids from cavitation may be due to the strokes of the slugs of liquid formed on collapse of cavities attached to the surface.

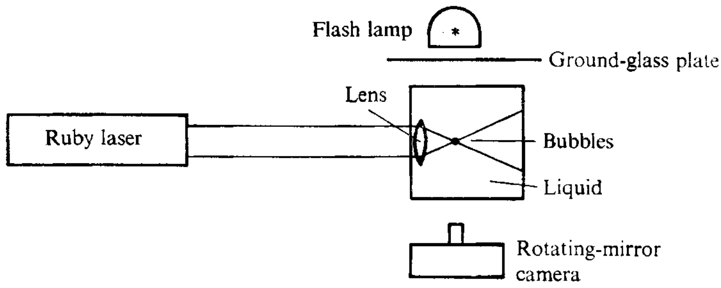

FIGURE 1. Schematic diagram of the set-up.

Since the first experimental evidence of jet formation (Naudé & Ellis 1961) many papers have appeared on this subject. To avoid repetition the reader is referred to two recent papers of Hammitt and co-workers to trace the historical development (Kling & Hammitt 1972; Mitchell & Hammitt 1973; see also Gibson 1968).

The present paper reports some measurements on cavitation bubbles near solid surfaces produced by a ruby laser. It has been shown that laser-produced cavitation bubbles offer unique possibilities of studying cavitation-bubble dynamics (Felix & Ellis 1971; Lauterborn 1974*a*, *b*). Extremely highly controlled conditions can be achieved, making sophisticated studies on cavitation-bubble collapse feasible. In particular, highly spherical bubbles can be produced exactly where wanted, free of mechanical destruction. Jet formation and the penetration of the bubble wall by the jet (bubble collapse) have been filmed with framing rates as high as 900000 frames/s (Lauterborn 1974*a*, *b*).

To get quantitative data (for instance jet velocities) the frames must be carefully analysed. The present paper describes our efforts and results in this direction. To cope with the amount of photographic material a computer-aided approach was tried. The bubble shape (analysed for each frame) was fed into a digital computer using a graphical input device. From these data, bubble-wall velocities were calculated. A special shape–time diagram is compared with the corresponding shape–time dependence calculated by Plesset & Chapman (1971), yielding remarkable agreement.

2. Apparatus

A schematic diagram of the most essential parts of the experimental set-up is shown in figure 1. Giant pulses emitted by a Q-switched ruby laser with a beam diameter of about 1 cm, a pulse duration of about 30–50 ns and a total pulse energy of about 0·1–1 J are focused into distilled water by means of a single lens with a focal length of 1·28 cm (when used in air, but 4·3 cm in water). The container used is a cube with an inner edge length of 10 cm. The bubbles produced in the vicinity of the focal point of the lens (in most cases submerged in the liquid) are diffusely illuminated by a flash lamp through a ground-glass plate and photographed by a Beckman–Whitley Model 330 rotating-mirror camera, which allows a maximum framing rate of about one million frames/s.

Under these backlighting conditions bubbles look dark on a bright background, with a bright central spot where the light passes through the bubble undeflected. For the sake of clarity, the electronics needed for timing the different activities of the devices have been omitted in the diagram as well as some auxiliary equipment like an He–Ne laser used for alignment of the optical components and the photographic apparatus.

3. Phenomena observed

A typical sequence of pictures of bubble growth, collapse and rebound taken with 75000 frames/s is shown in figure 2 (plate 1). The solid boundary, a brass plate at a variable distance from the location of bubble growth, is seen as a dark strip in the lower part of each frame. It appears somewhat blurred because it extends far out of the focal plane of the photographic system. The bubble was produced at a distance $b = 4 \cdot 9$ mm from the solid boundary and reached a maximum radius $R_{max} = 2 \cdot 0$ mm. Thus the ratio b/R_{max}, important for normalization, becomes 2·45. In the first frame the breakdown is seen as a bright spot, which leads to an initially extremely rapidly expanding bubble. At maximum size this bubble is almost exactly spherical. During collapse, it loses spherical symmetry by becoming elongated in the direction normal to the boundary. This elongation was predicted theoretically by Rattray as early as 1951 and was confirmed experimentally by Benjamin & Ellis in 1966. In the final stage of collapse a pronounced jet is produced, penetrating the bubble towards the boundary as a result of a higher collapse velocity of the upper bubble wall. This jet is directly visible as a fine dark line only in the bright central spot of the bubble after the first collapse. The funnel-shaped protrusion is a secondary effect produced by the jet through deformation of the lower bubble wall on impingement. The jet inside the protrusion is believed to be much thinner (like the fine dark line in the bright central spot). Also it is thought that the velocity of the tip is not the velocity of the jet. The jet will penetrate the bubble wall and thus have a higher velocity than the tip. So a distinction has to be made between the so-called 'tip velocity' and the 'true jet velocity'. Up to now it has been possible to measure only the tip velocity (see below).

In the second collapse the bubble starts as a deformed (non-spherical) bubble of a distinct shape: flattened at the top, elongated at the bottom and with a thin column of water connecting top and bottom. This special configuration, always obtained for an initially spherical cavitation bubble near a plane solid boundary, usually collapses with the formation of a jet in the opposite direction to the first jet. This jet can be detected in frames 3–6 in the lowest line of frames in figure 2. Jets directed away from the solid boundary will be called 'counterjets'.

The preceding description of bubble dynamics near a plane solid boundary is valid in the majority of cases investigated. But fairly often somewhat different behaviour of the bubble was observed as shown in figure 3 (plate 2). There only part of the whole bubble motion is shown, near the first collapse. The framing rate in this case is 300000 frames/s. In the first frame it can be seen that the bubble is elongated perpendicular to the boundary as usual. Then the bubble

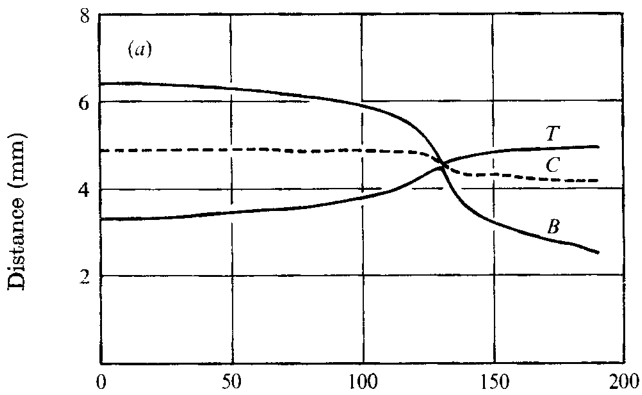

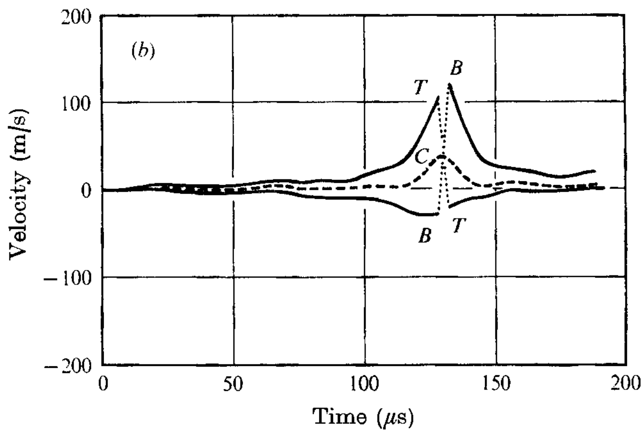

FIGURE 4. Bubble collapse near a solid wall evaluated from a film taken with a framing rate of 250000 frames/s and $b/R_{max} = 3{\cdot}08$. (*a*) Distance from the wall for different points of the bubble wall (T = top, C = centre, B = bottom of the bubble) *vs.* time. (*b*) Velocity of the three points *vs.* time.

top flattens and involutes, but after collapse a tiny jet (a 'counterjet') sticks out of the bubble in the opposite direction. The large jet towards the boundary develops on a much slower time scale. The counterjet extends a considerable distance out of the upper part of the bubble immediately after collapse. This is not due to a high velocity away from the boundary, but occurs because the bubble as a whole is suddenly driven towards the wall during collapse. A tiny counterjet is also visible in figure 2.

4. Measurements and data processing

To evaluate bubble motion from the films the distances of various parts of the bubble wall from the boundary have been determined with the aid of a digital computer and a graphical input device. The frames were projected onto a translucent plate of the input device and the co-ordinates (bubble wall and boundary) fed into the computer. Because of the blurred image of the bubble boundary in the frames the distance–time curves become rather rough. Therefore the curves were smoothed by the computer by a procedure which essentially consists of a low-pass filtering of the curves. Three of these curves are shown in figure 4(*a*), where T denotes the top of the bubble and B the bottom (after collapse it is the tip of the protrusion); C is the bubble centre (taken from the bright central spot on the bubble in the frames). The framing rate in this case is 250 000 frames/s and the ratio b/R_{max} is 3·08. The time is arbitrarily set to zero at the beginning of the plot. As derivatives can be taken from the smoothed curves in figure 4(*a*), the velocities of different points of the bubble wall can be calculated. They are plotted in figure 4(*b*) for the three cases of figure 4(*a*). Of course the velocity–time curves cannot be followed through the collapse for the top and the bottom of the bubble as there is a very rapid change in speed and the framing rate is too slow to follow the motion. The corresponding parts of the curves before and after collapse are therefore connected by a straight dotted line. The centre curve shows that the bubble is driven toward the boundary during the final stage of collapse and the first stage of rebound, with a maximum velocity of about 35 m/s, attained apparently at the actual point of collapse (figure 4*b*). The bubble develops a jet towards the boundary, as can be seen in figure 4(*a*) from the asymmetry of the top and bottom curves with respect to the centre curve after collapse. The tip velocity can be read from figure 4(*b*). A maximum velocity of about 120 m/s was calculated. As mentioned before, the true jet velocity is believed to be higher than this tip velocity by an amount not yet known. But in any case the experiments show that even bubbles far away from boundaries (in this case $b/R_{max} \approx 3$) may develop a strong jet (when undisturbed). From these experiments it is concluded that spherical shrinking of cavitation bubbles down to the actual point of collapse is highly improbable in any real situation, and that jet formation of cavitation bubbles on collapse is a normal process.

5. Comparison of bubble shape on collapse with theory

Figure 5 (plate 2) shows a section of a bubble collapsing near a solid boundary taken with a framing rate of 300 000 frames/s (only a small part of the film is shown here). The bubble has a maximum radius of $R_{max} = 2{\cdot}6$ mm and was produced at a distance from the boundary of $b = 3{\cdot}9$ mm, so that $b/R_{max} = 1{\cdot}5$. Thus a comparison of the bubble shape as a function of time with theoretical results obtained by Plesset & Chapman (1971) is possible. Plesset & Chapman have calculated the collapse of an empty, initially spherical cavity in the neighbourhood of a solid boundary for two cases: $b/R_{max} = 1$ and 1·5. The latter case, as already mentioned, is the one realized experimentally and thus can be compared with these calculations. As the instants at which pictures were taken do not coincide with those of the calculated curves, an interpolation was done to fit the calculated curves. Additional difficulties arose from the fact that, even at the framing rate of 300 000 frames/s applied, the instant of collapse cannot be determined precisely. Also, from the calculations it is not quite clear what instant should be taken as the final collapse. Thus a more or less arbitrary estimate of the instant of collapse, where the experimental and theoretical curves were fitted in time, was made, and then the shape of the bubble was

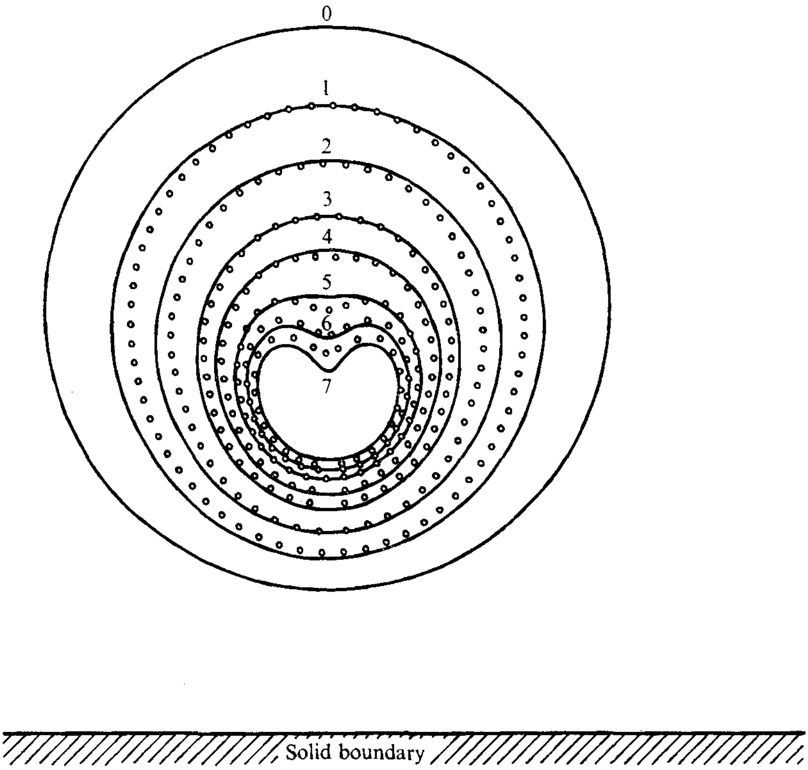

FIGURE 6. Comparison of experimentally determined bubble shapes (open circles) on collapse of a spherical bubble near a plane solid wall with theoretical curves taken from Plesset & Chapman (1971) (solid curves). The framing rate is 300000 frames/s, the maximum bubble radius $R_{max} = 2{\cdot}6$ mm, the distance of the bubble centre from the wall $b = 3{\cdot}9$ mm and $b/R_{max} = 1{\cdot}5$.

Curve	0	1	2	3	4	5	6	7
Time, $R_{max}(\rho_0/\Delta p)^{\frac{1}{2}}$	0	0·725	0·825	0·961	0·991	1·016	1·028	1·036

(ρ_0 is the density of the liquid and Δp is the constant difference between the ambient liquid pressure and the pressure in the cavity.)

compared backwards in time. The result is shown in figure 6. The open circles represent experimental data while the solid lines are taken from the calculations of Plesset & Chapman. The initial (experimental) bubble shape is not exactly spherical. But nevertheless the behaviour of the bubble (involution of the top and jet formation towards the boundary) fits the theory almost quantitatively.

6. Discussion

The dynamics of laser-induced cavitation bubbles in water near solid boundaries have been investigated by high-speed photography. Jetting effects could be studied in considerable detail. In the example reported here a maximum jet velocity (or, rather, tip velocity) of 120 m/s was measured at a framing rate of 250000 frames/s and a value of $b/R_{max} = 3{\cdot}08$ (figure 4). The measured tip velocities depend on the framing rate used. They are higher the higher the framing rate. This implies that the value of 120 m/s observed here is a lower bound to actually occurring velocities. Kling & Hammitt (1972) have also found a maximum tip velocity of 120 m/s using spark-produced bubbles, but at $b/R_{\max} = 1{\cdot}14$ and taken at impingement of the jet (tip of the protrusion) on the solid surface (called the jet impingement velocity). As the maximum jet velocity in a particular collapse will occur on impingement of the jet on the opposite wall of the bubble, the maximum jet velocity of the bubble Kling & Hammitt have examined must have been higher, as is indicated by the frames shown. Unfortunately it is not known whether the frames in the paper of Kling & Hammitt are from one bubble only or from different sequences of similar bubbles. We believe that only velocity measurements on the same bubble as made here will yield reliable lower bounds to the jet velocity.

Experiments using framing rates higher than those in the experiments reported here are really needed to settle the question of the jet velocities occurring on cavitation-bubble collapse. As it seems possible to trigger the moment of collapse of a laser-induced cavitation bubble, studies of bubble collapse with framing rates of several million or even some ten million frames per second seem feasible.

Besides 'normal' jet formation towards the solid boundary, jet formation away from the boundary was observed in the experiments (figures 2 and 3). This has not been predicted theoretically, but was easily observable in these experiments. There seem to be two types of counterjets, one occurring on the first collapse, the other on the second collapse. The counterjet occurring on the first collapse is extremely thin compared with the main jet towards the boundary. It develops extremely fast (within several microseconds), at least ten times faster than the main jet, on the basis of the time necessary to reach maximum size. The counterjet developing on the second collapse is much larger than the first counterjet and has a flat 'tip': no high velocities seem to be involved.

It is not known whether the counterjet formation is a deficiency of the bubble production method or whether it is inherent in bubble dynamics near solid boundaries. The idea that the bubble production method may be the cause of the counterjets (especially the first one) arises from the fact that a strong shock wave is radiated on bubble formation (Felix & Ellis 1971) and is reflected back from the solid boundary. This introduces asymmetry into the flow around the bubble during bubble growth within the first few microseconds. There is nothing detectable in the shape of the bubble but nevertheless the disturbance may persist during growth and manifest itself on collapse. This explanation may be transferred to the second counterjet through the argument that, on the first collapse, a strong shock wave is again radiated. This argument would leave the counterjet formation both a deficiency of the method and an inherent part of bubble dynamics near solid boundaries.

Another observation, which the authors feel may help towards a theoretical explanation, is that jet formation appears to be related to the curvature of the bubble wall. More precisely, it is observed that more highly curved parts of a bubble collapse faster than less curved parts (see also Lauterborn 1974*a*).

Of course this relation will hold only under special conditions. No theory has yet been developed to verify the conjectured relation and to give the limits of its validity. Nor has its consistency, or otherwise, with previously published theoretical arguments been checked. But the numerical calculations of Chapman & Plesset (1972) indicate that it will hold for a large class of configurations. Chapman & Plesset have calculated the collapse of two types of initially non-spherical bubbles (elongated and flattened like the earth). In both cases the more highly curved parts collapse faster than the less curved parts, exactly as is observed in experiments (Bolle 1974). Of course the authors do not expect the relation to remain valid if a liquid flow which is not due to the bubble motion itself is imposed around the bubble.

Consistent with the above hypothesis is the fact that the counterjets are seen to develop from more highly curved parts of the bubble wall. As the bubble first becomes elongated in the direction normal to the wall, the top and bottom should develop a jet. But at the bottom obviously there is a competition between the higher curvature and the influence of the solid boundary. As the experiments show, the effect of the higher curvature may take over in the final stage of collapse, giving rise to the counterjet. It is believed that this jet can appear only when there is some asymmetry present in the bubble motion, so that the main jet cannot tear it along (because of its higher velocity and larger dimensions). This is supported by the observation that in all cases where such a counterjet is observed the main jet is grossly distorted and does not develop very well.

It is interesting to note that counterjets can be found in frames in the paper of Kling & Hammitt (1972). But no attention is paid to this phenomenon, perhaps because the spark-generated bubbles usually have a rather rough surface and the counterjets thus are not the only irregularity in the shape observed. But their occurrence in spark-generated bubbles too supports the idea that counterjet formation may be another distinct feature besides jet formation of the dynamics of a bubble near a solid boundary.

Theory can predict so far the collapse of a bubble until the jet strikes the opposite wall of the bubble (Plesset & Chapman 1971). This part of the bubble history has been compared with experiments (figures 5 and 6). Remarkable agreement was found. At the time of which the calculations were done it seemed impossible to verify them by experiment ("Experiments are difficult and give only sketchy results," Plesset & Chapman 1971). This general feeling in cavitation research was due to the fact that bubble production methods suitable for systematic investigations were lacking. As shown in this paper, especially in the comparison with the calculations (figure 6), many of the experimental difficulties can be overcome by using laser-produced bubbles. Extremely spherical bubbles undisturbed by mechanical components of the bubble production mechanism can be produced in the bulk of the liquid. The bubbles Benjamin & Ellis (1966) used in their experiments show the same properties, but obviously were much more difficult to handle. After their electrolytic generation and rising in the liquid to the proper position, they had to be expanded before collapse could be observed. Laser-produced bubbles are simply formed by focusing the light at the position where they are wanted. The deficiencies of this method are the difficulty of obtaining just one single spherical bubble of precisely the size wanted and the strong shock wave that is radiated on bubble formation.

But these deficiencies can be used to study bubble interaction (Lauterborn 1974*a*; Bolle 1974) and shock-wave/bubble interaction (Lauterborn 1972, 1974*a*)

7. Conclusions

The main results of this paper are as follows.

(i) Numerical calculations of bubble collapse near solid boundaries were quantitatively confirmed by experiments.

(ii) Jet (tip) velocities could be measured with great precision.

(iii) The generation of cavitation bubbles by laser light proves to be a unique and important tool in cavitation physics. Besides hydraulic cavitation and acoustic cavitation a new area may open up called *optical cavitation.*

The work on laser-produced bubbles reported here was supported by the Deutsche Forschungsgemeinschaft and the Fraunhofer-Gesellschaft. The experiments with the rotating-mirror camera were done at the Institut für den Wissenschaftlichen Film in Göttingen. The calculations were done on the Honeywell H 632 digital computer donated by the Stiftung Volkswagenwerk to the Third Physical Institute.

REFERENCES

BENJAMIN, T. B. & ELLIS, A. T. 1966 The collapse of cavitation bubbles and the pressures thereby produced against solid boundaries. *Phil. Trans.* A **260**, 221–240.

BOLLE, H. 1974 Nichtsymmetrischer Kollaps lasererzeugter Kavitationsblasen. Candidate dissertation, University of Göttingen.

CHAPMAN, R. B. & PLESSET, M. S. 1972 Nonlinear effects in the collapse of a nearly spherical cavity in a liquid. *J. Basic Engng, Trans. A.S.M.E.* D **94**, 142–146.

FELIX, M. P. & ELLIS, A. T. 1971 Laser-induced liquid breakdown – a step-by-step account. *Appl. Phys. Lett.* **19**, 484–486.

GIBSON, D. C. 1968 Cavitation adjacent to plane boundaries. *Proc. 3rd Conf. Hydraul. Fluid Mech., Sydney*, pp. 210–214. Austr. Inst. Engrs.

KLING, C. L. & HAMMITT, F. G. 1972 A photographic study of spark-induced cavitation bubble collapse. *J. Basic Engng, Trans. A.S.M.E.* D **94**, 825–833.

KORNFELD, M. & SUVOROV, L. 1944 On the destructive action of cavitation. *J. Appl. Phys.* **15**, 495–506.

LAUTERBORN, W. 1972 High-speed photography of laser-induced breakdown in liquids. *Appl. Phys. Lett.* **21**, 27–29.

LAUTERBORN, W. 1974*a* Kavitation durch Laserlicht. *Acustica,* **31**, 51–78.

LAUTERBORN, W. 1974*b* General and basic aspects of cavitation. In *Proc.* 1973 *Symp. Finite-Amplitude Wave Effects in Fluids, Copenhagen* (ed. L. Bjørnø), pp. 195–202. Guildford, England: IPC Science and Technology Press.

MITCHELL, T. M. & HAMMITT, F. G. 1973 Asymmetric cavitation bubble collapse. *J. Fluids Engng, Trans. A.S.M.E.* I **95**, 29–37.

NAUDÉ, C. F. & ELLIS, A. T. 1961 On the mechanism of cavitation damage by nonhemispherical cavities collapsing in contact with a solid boundary. *J. Basic Engng, Trans. A.S.M.E.* D **83**, 648–656.

PLESSET, M. S. & CHAPMAN, R. B. 1971 Collapse of an initially spherical vapour cavity in the neighbourhood of a solid boundary. *J. Fluid Mech.* **47**, 283–290.

RATTRAY, M. 1951 Perturbation effects in bubble dynamics. Ph.D. dissertation, California Institute of Technology.

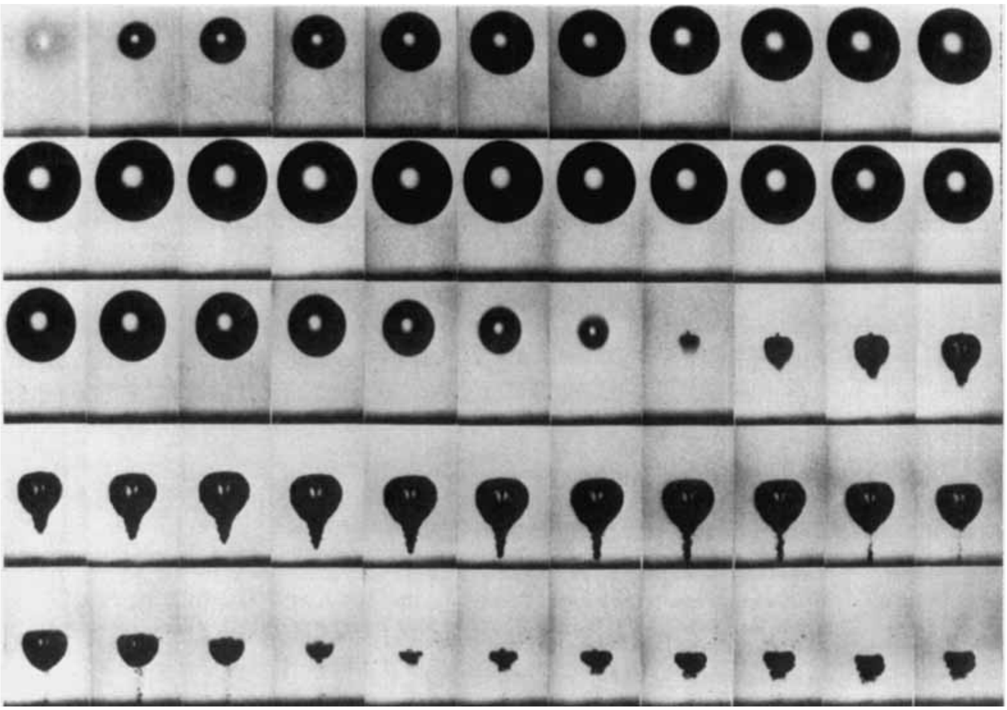

FIGURE 2. Dynamics of a laser-produced spherical bubble near a solid boundary. The framing rate is 75000 frames/s, the maximum bubble radius $R_{max} = 2 \cdot 0$ mm, the distance of the bubble centre from the boundary $b = 4 \cdot 9$ mm and the size of the individual frames is $7 \cdot 2 \times 4 \cdot 6$ mm.

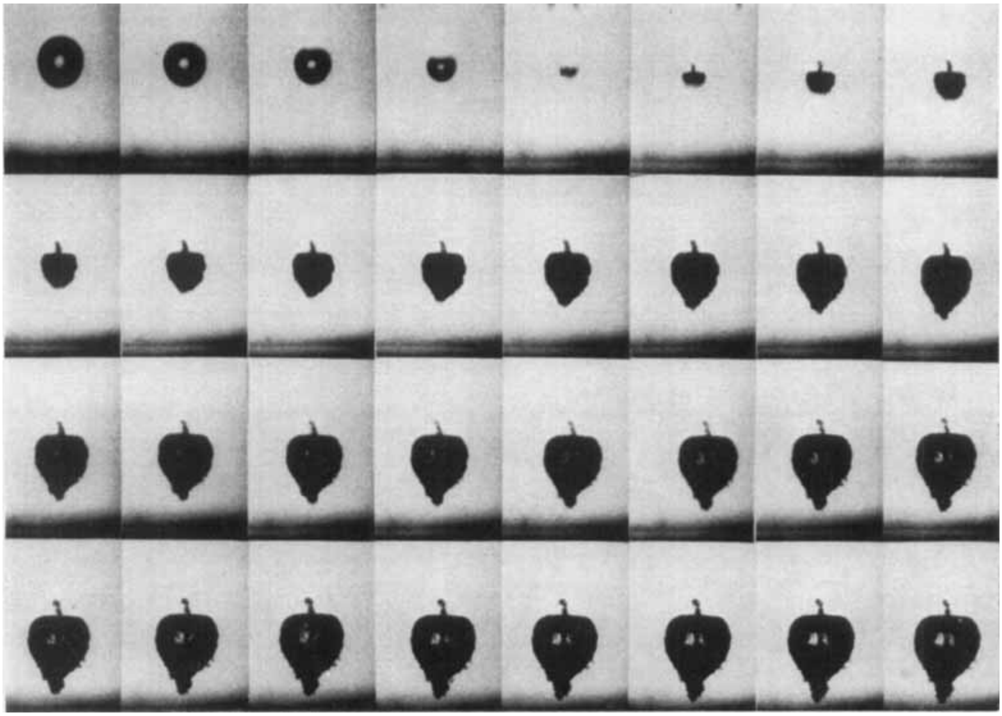

FIGURE 3. Bubble collapse and rebound near a solid boundary. The framing rate is 300000 frames/s and the size of individual frames is 5·6 × 3·9 mm.

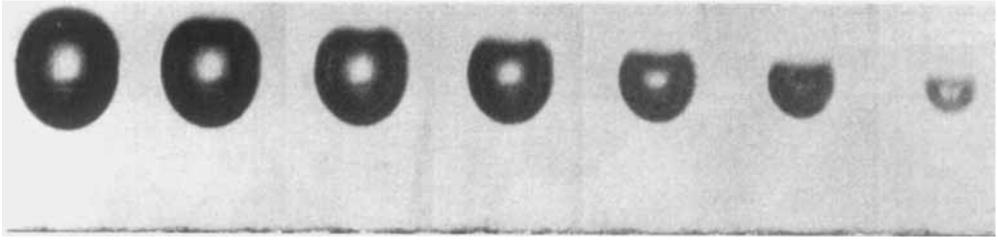

FIGURE 5. Section of the collapse phase of a cavitation bubble near a plane solid wall. The framing rate is 300000 frames/s and the size of individual frames is 4·9 × 3·0 mm.